Author/s:
Chen, X;Yan, Y;Müllner, M;Ping, Y;Cui, J;Kempe, K;Cortez-Jugo, C;Caruso, F

Title:
Shape-Dependent Activation of Cytokine Secretion by Polymer Capsules in Human Monocyte-Derived Macrophages

Date:
2016-03-14

Citation:
Chen, X., Yan, Y., Müllner, M., Ping, Y., Cui, J., Kempe, K., Cortez-Jugo, C. & Caruso, F. (2016). Shape-Dependent Activation of Cytokine Secretion by Polymer Capsules in Human Monocyte-Derived Macrophages. Biomacromolecules, 17 (3), pp.1205-1212. https://doi.org/10.1021/acs.biomac.6b00027.

Persistent Link:
https://hdl.handle.net/11343/108746

Shape-Dependent Activation of Cytokine Secretion by Polymer Capsules in Human Monocyte-Derived Macrophages

*Xi Chen, Yan Yan, Markus Müllner, Yuan Ping, Jiwei Cui, Kristian Kempe, Christina Cortez-Jugo, and Frank Caruso**

[†]ARC Centre of Excellence in Convergent Bio-Nano Science and Technology, and the Department of Chemical and Biomolecular Engineering, The University of Melbourne, Parkville, Victoria 3010, Australia.

ABSTRACT: Particles with tailored geometries have received significant attention due to their specific interactions with biological systems. In this work, we examine the effect of polymer capsule shape on cytokine secretion by human monocyte-derived macrophages. Poly(methacrylic acid) (PMA_{SH}) polymer capsules with different shapes (spherical, short rod-shaped, and long rod-shaped) were prepared by layer-by-layer assembly. The effect of PMA_{SH} capsule shape on cellular uptake and cytokine secretion by macrophages differentiated from THP-1 monocytes (dTHP-1) was investigated. PMA_{SH} capsules with different shapes were internalized to a similar extent in dTHP-1 cells. However, cytokine secretion was influenced by capsule geometry: short rod-shaped PMA_{SH} capsules promoted a stronger increase in TNF-α and IL-8 secretion compared

with spherical (1.7-fold in TNF-α and 2.1-fold in IL-8) and long rod-shaped (2.8-fold in TNF-α and 2.0-fold in IL-8) PMA_{SH} capsules in dTHP-1 cells. Our results indicate that the immunological response based on the release of cytokines is influenced by the shape of the polymer capsules, which could be potentially exploited in the rational design of particle carriers for vaccine delivery.

INTRODUCTION

Over the past decade, synthetic particles have received significant attention in vaccinology, either as delivery systems to improve antigen processing or as immunostimulators to activate immunity.[1-3] Various engineered particles, including virus-like particles,[4] lipid particles,[5] inorganic particles,[6] and polymeric particles,[7] have shown different immune-modulatory activities (including inflammation-related cytokine secretion), which subsequently regulate immunological responses. Polymer capsules fabricated through layer-by-layer (LbL) assembly on template particles are regarded as promising candidates for vaccine delivery due to their multifunctional surface chemistries, controllable and tunable morphology, and cargo loading/release properties.[8-10] We previously reported the loading of oligopeptide vaccines into LbL polymer capsules and demonstrated the delivery of functionally active cargo to antigen presenting cells to stimulate immune responses.[11] In addition, ovalbumin (OVA) proteins/peptides encapsulated in polymer capsules were shown to stimulate T cell immunity more effectively than OVA protein administered alone, which highlights the in vivo potential of polymer-based vaccine delivery technologies.[12] These studies demonstrate the potential application of polymer capsules for effective vaccine delivery and vaccine adjuvants that boost

immunogenicity. Hence, elucidating the fundamental effect of polymer capsule physicochemical properties on the immunological response is essential for their further development in vaccinology.

Physicochemical properties, including size,[13,14] shape,[15] ligand density,[16] surface charge[17] and rigidity,[18,19] are recognized as important parameters that govern the behavior of micro-/nanoparticles in the biological domain.[20] Particle shape has recently been emphasized as a key parameter that influences cellular uptake in different cell lines.[21,22] For example, HeLa cells showed shape-dependent cellular uptake, where spherical gold nanoparticles (D = 14 nm or 74 nm) were internalized to a greater extent than rod-shaped nanoparticles (74 × 14 nm).[23] In contrast, mesoporous silica nanoparticles showed a reverse trend, with rod-shaped particles (450 × 110 nm) more efficiently internalized by human melanoma cells compared to spherical particles (D = 100 nm).[24] Recently, we synthesized rod-shaped polymer capsules with different aspect ratios (AR 1-4) and demonstrated that their cellular uptake by HeLa cells became slower with increasing AR.[25] The differences in the cellular endocytic pathway in different cell lines may dictate the type of interaction between particles and cells. Therefore, the effect of particle shape on cellular uptake is expected to be a broad interplay of particle geometry and surface chemistry, as well as the type of cell being investigated.[26] Beyond the effect of particle shape on cellular uptake, there are few reports on the effect of particle shape on immunological responses, although this factor is critical for both in vitro and in vivo applications. Maysinger et al. first reported the effect of gold nanoparticle (AuNP) shape on the inflammatory response in microglial cells.[27] For example, poly(ethylene glycol)-coated spherical (D = 23 nm) and rod-shaped (43 × 12 nm) AuNPs stimulated the release of granulocyte macrophage colony-

stimulating factor (GM-CSF), while urchin-shaped (D = 77 nm) AuNPs significantly reduced GM-CSF secretion to barely detectable levels. Recently, Niikura et al. reported that rod-shaped AuNPs (36 × 10 nm) significantly induced the production of interleukin (IL)-1β and IL-18 at different levels in dendritic cells.[6] However, spherical (D = 43 nm) and cubic (D = 41 nm) AuNPs triggered the secretion of other types of cytokines (tumor necrosis factor alpha (TNF-α), IL-6, IL-12 and GM-CSF). These differences in cytokine secretion in response to particles with different morphology suggest that immunological responses can be modulated by the shape of the particles.

Herein, we report the effect of polymer capsule shape on cytokine secretion by differentiated macrophage-like THP-1 cells (dTHP-1). Thiolated poly(methacrylic acid) (PMA_{SH}) capsules with different shapes [spherical (D = 670 nm, AR 1.0), short rod-shaped (720 × 330 nm, AR 2.2), and long rod-shaped (2250 × 305 nm, AR 7.4)] were fabricated via LbL assembly on template silica (SiO_2) particles, and the effect of PMA_{SH} capsule shape on cellular association, internalization, and cytokine secretion by dTHP-1 cells was investigated. THP-1 is a human acute leukemia cell line that has been commonly used as an in vitro model of monocytes and macrophages in the investigation of immune modulation.[28] THP-1 cells are monocytic, but can be differentiated into macrophage-like cells (dTHP-1) via incubation with phorbol 12-myristate 13-acetate (TPA), which activates protein kinase C and leads to enhanced phagocytotic capability and the expression of surface macrophage markers.[29] Our results show that PMA_{SH} capsules with different shapes were similarly internalized in dTHP-1 cells, regardless of their shape. However, we observed that cytokine secretion of TNF-α and IL-8 by dTHP-1 cells was influenced by the shape of PMA_{SH} capsules: short rod-shaped PMA_{SH} capsules promoted a

higher increase in TNF-α and IL-8 secretion compared with spherical (1.7-fold in TNF-α and 2.1-fold in IL-8) and long rod-shaped (2.8-fold in TNF-α and 2.0-fold in IL-8） PMA_{SH} capsules in dTHP-1 cells. These results demonstrate that the shape of the polymer capsule can influence the immunological response in macrophage-like cells.

EXPERIMENTAL SECTION

Materials. Spherical silica (SiO_2, D = 500 nm) particles were purchased from Micro-Particles GmbH (Berlin, Germany). 1-(3-Dimethylaminopropyl)-3-ethylcarbodiimide (EDC), tetraethyl orthosilicate (TEOS), sodium acetate (NaOAc), phosphate-buffered saline (PBS), chloramineT (CaT), hydrofluoric acid (HF), poly(vinylpyrrolidone) (PVPON, M_w 10 and 40 kDa), 4-(4,6-dimethoxy-1,3,5-triazin-2-yl)-4-methylmorpholinium chloride (DMTMM), dithiothreitol (DTT), 3-(*N*-morpholino)-propanesulfonic acid (MOPS), 2-morpholinoethanesulfonic acid (MES), 1-pentanol, 12-*O*-tetradecanoylphorbol-13-acetate (TPA) were purchased from Sigma-Aldrich and used as received. Poly(methacrylic acid) sodium salt (PMA, M_w= 15 kDa) was purchased from Polysciences, Inc. (Warrington, USA). Pyridine dithioethylamine hydrochloride (PDA-HCl) was purchased from Shanghai Speed Chemical Co. Ltd. (China). Alexa Fluor 488 wheat germ agglutinin (AF488 WGA), Alexa Fluor 633 hydrazide (AF633) and Alexa Fluor 488 goat anti-mouse IgG were purchased from Invitrogen (Life Technologies Australia, Pty. Ltd.). Ammonia solution (25 wt%) and propidium iodide (PI) were purchased from Merck. Sodium citrate dihydrate was obtained from Fluka (Sigma-Aldrich) . Cell culture media Roswell Park Memorial Institute (RPMI) 1640 containing GlutaMax, heat-inactivated fetal bovine serum (HI-FBS), Dulbecco’s phosphate-buffered saline (DPBS) were

purchased from Life Technologies Australia, Pty. Ltd.). Mouse anti-human LAMP-1 antibody (CD107a) was purchased from BD Pharmingen. Ethanol (absolute) was obtained from Chem-Supply (Australia). Highly purified water with resistivity greater than 18.0 MΩ·cm obtained from a Millipore Milli-Q purification system was used. Human TNF-α ELISA Kit, Human IL-6 ELISA Kit, Human IL-8 ELISA Kit, Human IL-18 ELISA Kit, Human IFN-γ ELISA Kit and Human IL-1β ELISA Kit were purchased from Thermo Fisher Scientific Inc.

Preparation of SiO_2 Rods. SiO_2 rods were fabricated according to the method reported by Kuijk et al.[30] Briefly, 30 g of PVPON (M_w 40 kDa) was dissolved in 300 mL of 1-pentanol by sonication for 4–6 h. Then, 8.4 mL of Milli-Q water, 2 mL of sodium citrate dihydrate solution (0.18 M in water), 30 mL of absolute ethanol and 6.75 mL of ammonia were added to the mixture. The solution was mixed by gentle inversion for 1 min, and then allowed to stand for 5 min before the addition of 3 mL of TEOS. The reaction mixture was mixed again by gentle inversion for 1 min, and then allowed to proceed at 37 ˚C for different time intervals with no mixing. SiO_2 rods with AR 2.5 (short rod-shaped templates) and AR 13 (long rod-shaped templates) were prepared by incubating for 20 min and 80 min, respectively. To purify the rods, the middle layer of the reaction mixture was collected and centrifuged at 3000 *g* for 60 min. The pellet was washed twice with ethanol, then twice with Milli-Q water before resuspension in Milli-Q water.

Preparation of Thiolated PMA (PMA_{SH}). Poly(methacrylic acid) modified with 9% thiol groups was synthesized as reported elsewhere.[31] Briefly, PMA solution (187.15 mg of 30 wt% solution) was diluted with 2 mL of phosphate buffer (10 mM, pH 7.3). The resulting solution was pre-catalysed with 43 mg of EDC, and the mixture was stirred at ambient temperature for 10

min. PDA–HCl (28.36 mg) was added to the mixture, and the reaction was allowed to proceed for 12 h. The resulting solution was purified via dialysis for 3 days against Milli-Q water and freeze dried overnight to obtain PMA–PDA in powder form. The extent of thiol modification of PMA was quantified using a NanoDrop 1000 spectrophotometer (Thermo Scientific). To expose thiol groups, PMA–PDA was incubated with 0.5 M DTT in MOPS buffer (20 mM, pH 8) to a concentration of 100 g L^{-1} for 15 min at 37 ˚C with shaking. The stock solution was then diluted with NaOAc buffer (50 mM, pH 4) to the desired concentration prior to LbL assembly.

Fabrication of PMA_{SH} Capsules. 5 mg of SiO_2 particles (spherical, short rod- and long rod-shaped particles) were washed three times by vortexing for 1 min, followed by centrifugation at 1000 *g* for 2 min and redispersion in NaOAc buffer (50 mM, pH 4). The particles were then resuspended in 50 µL NaOAc buffer by vortexing and sonication for 5 min. PVPON solution (50 µL at 4 g L^{-1} in 50 mM NaOAc buffer) was subsequently added to the SiO_2 particle suspension, followed by mixing for 10 min to allow for polymer adsorption. After incubation, the polymer-coated particles were washed by three cycles of centrifugation (1000 *g* for 2 min) and redispersion in NaOAc buffer, and finally resuspended in 50 µL NaOAc buffer. PMA_{SH} solution (50 µL at 4 g L^{-1} in 50 mM NaOAc buffer) was then added to the PVPON-coated particles and incubated for 10 min. The particles were washed as described above and resuspended in 50 µL NaOAc buffer. The sequential adsorption of PVPON and PMA_{SH} was repeated until 4 bilayers ($(PVPON/PMA_{SH})_4$) were deposited on the particles. The PMA layers were crosslinked through the formation of disulfide bonds. Briefly, the polymer-coated particles were exposed to 2.8 mM of CaT in MES buffer (50 mM, pH 6) and incubated with gentle shaking overnight. The resulting disulfide-stabilized core-shell particles were washed by two centrifugation and redispersion

cycles in MES buffer, and two washing cycles in NaOAc buffer. Capsules were obtained by dissolving the SiO_2 templates using 5 M HF for 5 min (*Caution! HF is highly toxic and extreme care must be taken when handling it!*), followed by three washing cycles of centrifugation and resuspension in PBS buffer. During this washing step, sacrificial PVPON polymer layers were also removed, resulting in pure PMA_{SH} capsules. The capsules were fluorescently labeled by incubation with 5 µL AF633 hydrazide (1 g L^{-1}) and 1 mg DMTMM in 200 µL PBS for 6 h, followed by washing and redispersion in PBS four times.

Characterization of PMA_{SH} Capsules. Fluorescently labeled PMA_{SH} capsules were imaged on an inverted fluorescence microscope (Olympus IX71) equipped with a cyanine 5 filter cube. Transmission electron microscopy (TEM, Philips CM120 BioTWIN, operated at 120 kV) was used to study the morphologies of the SiO_2 templates and capsules at high resolution. The polymer shell thickness of the PMA_{SH} capsules was measured by atomic force microscopy (AFM) using ultrasharp SiN gold-coated cantilevers (NT-MDT) on a MFP-3D AFM (Asylum Research) using AC mode. Capsule concentration was determined with an Apogee flow cytometer (A50-Micro, Apogee Flow Systems Ltd.) using an excitation wavelength of 638 nm (Figure S1).

Cell Culture. Human monocytic leukemia cell line THP-1 cells were maintained in suspension in complete RPMI medium (RPMI-1640 containing 10% fetal bovine serum, termed as cRPMI) at 37 ˚C in a 5% CO_2 humidified atmosphere. An adherent macrophage-like version of THP-1 (dTHP-1) was obtained by incubation of THP-1 cells with 200 nM TPA for 48 h in cRPMI medium.

Cellular Association of PMA_{SH} Capsules. dTHP-1 cells were plated into 24-well plates at 1×10^5 cells per well, and incubated overnight. Subsequently, PMA_{SH} capsules (spherical, short rod- and long rod-shaped capsules) were added at a cell-to-capsule ratio of 1:100 and incubated at 37 ˚C in 5% CO_2 for 2, 6, 16 and 24 h. At each timepoint, dTHP-1 cells were harvested by trypsinization at 37 ˚C and washed with DPBS three times by centrifugation/redispersion cycles at 300 *g* for 5 min. The cells were resuspended in DPBS and at least 8000 cells were analyzed by flow cytometry (A50-Micro, Apogee Flow Systems Ltd.).

Cellular Viability Assay. The viability of cells after incubation with PMA_{SH} capsules was examined by propidium iodide (PI) treatment. Capsules were prepared as described above. dTHP-1 cells were incubated with PMA_{SH} capsules at a cell-to-capsule ratio of 1:100 for 24 h at 37 ˚C in 5% CO_2. After incubation, the cells were collected, washed with DPBS, and resuspended in DPBS containing 0.025 mg/mL PI for 30 min in the dark at room temperature. The fluorescence intensity of PI treated cells was analyzed by flow cytometry (A50-Micro, Apogee Flow Systems Ltd.), using laser excitation wavelength of 552 nm.

Cellular Internalization of PMA_{SH} Capsules. dTHP-1 cells were plated in 6-well plates at 5×10^5 cells per well, and incubated overnight. PMA_{SH} capsules at a cell-to-capsule ratio of 1:100 were added, and incubated for 16 h at 37 ˚C in 5% CO_2. After treatment, dTHP-1 cells were harvested by trypsinization at 37 ˚C and washed with DPBS three times by centrifugation/redispersion cycles at 300 *g* for 5 min. Plasma membrane staining of the cells was carried out by incubating cells with AF488-WGA (0.5 µg/mL) at 4 ˚C for 15 min, followed by washing with cold DPBS three times by centrifugation/redispersion cycles at 300 *g* for 5 min. The cell pellet was resuspended in DPBS and analyzed by imaging flow cytometry (Amnis

ImageStream flow cytometer). Brightfield and fluorescence images of 5000 cells were acquired. The internalization analysis was performed using a built-in internalization feature of the Amnis ImageStream IDEAS software on single focused images of cells associated with capsules.

Cytokine Assay. dTHP-1 cells were incubated with PMA_{SH} capsules (spherical, short rod- and long rod-shaped capsules) at cell-to-capsule ratios of 1:25, 1:50 and 1:100 for 24 h at 37 ˚C. After treatment, the cell culture media was collected and then centrifuged at 6000 *g* for 5 min to remove any remaining capsules. Levels of TNF-α, IL-6, IL-8, IL-18, IFN and IL-1*β* in the supernatant were measured by standard ELISA kits as per the manufacturer's instructions.

Intracellular Fate. dTHP-1 cells were obtained from THP-1 cells after 48 h differentiation as described above, and plated at a density of 5×10^4 cells per well into 8-well Lab-Tek I chambered coverglass slides (Thermo Fisher Scientific, Rochester). dTHP-1 cells were then incubated with AF633-labeled PMA_{SH} capsules of different shapes at a cell-to capsule ratio of 1:100 (at 37 ˚C, 5% CO_2). After 24 h incubation, cells were fixed with 3% paraformaldehyde for 30 min at ambient temperature and washed with DPBS three times. To permeabilize the cell membrane for intracellular immunostaining, the fixed cells were incubated with 500 μL Triton X-100 (0.1% in PBS buffer) for 5 min at ambient temperature. Cell nuclei was stained with 200 μL Hoechst 33342 (1 μg mL^{-1}) for 15 min at ambient temperature. Late endosomes and lysosomes were immunostained with 200 μL mouse anti-human LAMP-1 antibody (CD107a) (2.5 μg mL^{-1}) for 45 min at ambient temperature. After washing, cells were incubated with 200 μL of secondary Alexa Fluor 488 goat anti-mouse IgG (2 μg mL^{-1}) for 45 min at ambient temperature. Fluorescence images were collected using deconvolution fluorescence microscopy (DeltaVision, Applied Precision) equipped with a 60× 1.42 NA oil objective and a standard

FITC/CY5 filter set. Images were processed with Imaris 6.3.1 (Bitplane) using a maximum intensity projection.

RESULTS AND DISCUSSION

Preparation and Characterization of PMA_{SH} Capsules. To obtain PMA_{SH} capsules with different shapes, SiO_2 templates (spherical shape, short rod-shaped and long rod-shaped templates; Figure S2) were sequentially coated with PMA_{SH}/poly(N-vinylpyrrolidone) (PVPON) through LbL assembly under acidic conditions (pH 4), followed by oxidative crosslinking of PMA_{SH} thiol groups into bridging disulfide linkages. PMA_{SH} capsules were obtained after dissolution of the SiO_2 templates in hydrofluoric acid and removal of the sacrificial PVPON layers by washing at pH 7.4. Transmission electron microscopy (TEM) images reveal spherical PMA_{SH} capsules retained their spherical shape after template removal (Figure 1, A1). However, the diameter of the spherical capsules, which were prepared using 500 nm SiO_2 templates, increased to approximately 670 nm (volume = 12.6×10^8 nm^3). This increase was expected because of the typical swelling of PMA capsules in aqueous suspensions when the pH is greater than the pK_a of PMA. Similarly, rod-shaped PMA_{SH} capsules remained rod-like in shape after template removal (Figure 1, A2 and A3); however, the swelling decreased the AR of the capsules: short rod-shaped capsules decreased from AR 2.5 (template) to AR 2.2 (720 × 330 nm, volume = 2.46×10^8 nm^3), and long rod-shaped capsules decreased from AR 13 (template) to AR 7.4 (2250 × 305 nm, volume = 6.58×10^8 nm^3). The size parameters of the capsules are summarized in Table S1 (in Supporting Information). Atomic force microscopy (AFM)

measurements show that the film thickness of PMA_{SH} capsules with four bilayers is 28 ± 5 nm for all shapes (Figure 1, B1-B3), resulting in an average thickness of 3.5 ± 0.6 nm per polymer layer (Figure S3). Alexa Fluor 633 (AF633)-labeled PMA_{SH} capsules with different shapes were also imaged by fluorescence microscopy, and minimal aggregation was observed upon exposure of the capsules to cell culture media (Figure 1, C1-C3). The capsule dispersions were further examined using flow cytometry (Figure S4), also indicating minimal aggregation.

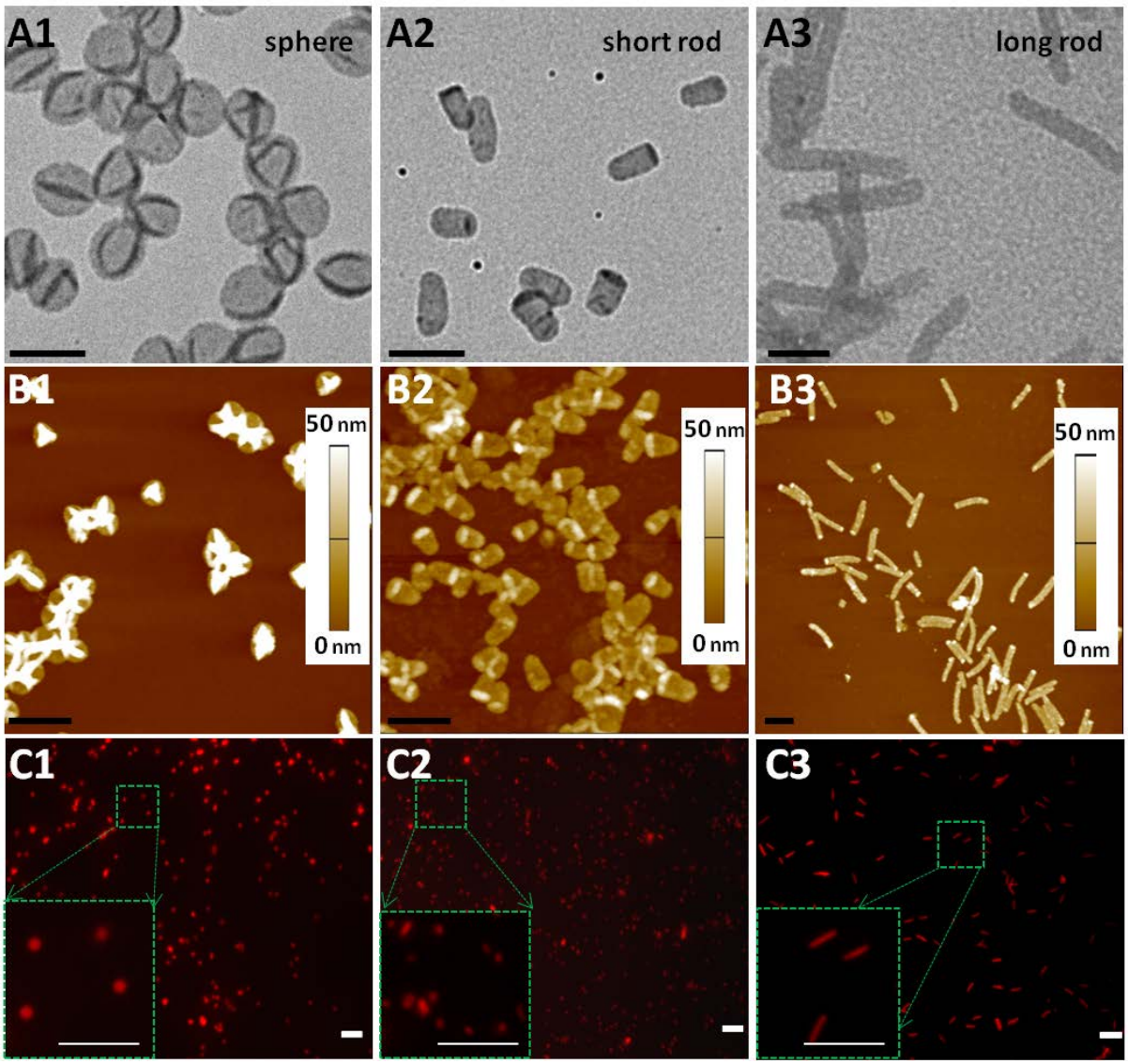

Figure 1. Respective TEM (A), AFM (B), and fluorescence microscopy (C) images of PMA_{SH} capsules with different shapes: **(A1, B1, C1)** spherical PMA_{SH} capsules; **(A2, B2, C2)** short rod-shaped PMA_{SH} capsules; and **(A3, B3, C3)** long rod-shaped PMA_{SH} capsules. Scale bars: A1-A3, 1 μm; B1-B3, 2 μm; and C1-C3, 5 μm.

Cell Association and Internalization. The effect of polymer capsule shape on cell association was investigated by incubating dTHP-1 cells with PMA_{SH} capsules at a capsule-to-cell ratio of 100:1 for 24 h at 37 ˚C. The concentration of the polymer capsules (absolute count per volume) was quantified using the Apogee A50-Micro flow cytometry system. The cell association kinetics was also monitored using flow cytometry and revealed a time-dependent process with a gradual increase in association as incubation time increased (Figure 2A). Figure 2A also shows that capsule shape had negligible influence on cellular association for dTHP-1 cells. The cellular uptake of PMA_{SH} capsules with different shapes by dTHP-1 cells after each time point was further confirmed by deconvolution fluorescence microscopy (Figure 2B). The images suggest that the cellular uptake for dTHP-1 cells was largely independent of PMA_{SH} capsule shape, where different shapes or ARs did not result in a significant difference in cellular association.

The capsules appeared to show excellent biocompatibility with dTHP-1 cells, as shown by the propidium iodide (PI) viability assay. PI is a fluorescent dye excluded from viable cells, but can penetrate cell membranes of dead or dying cells. Figure S5 shows the viability of dTHP-1

cells after 24 h incubation with PMA_{SH} capsules at 37 ˚C. The cells exhibited high viability, even at a capsule to cell ratio of 100:1, regardless of capsule shape.

A

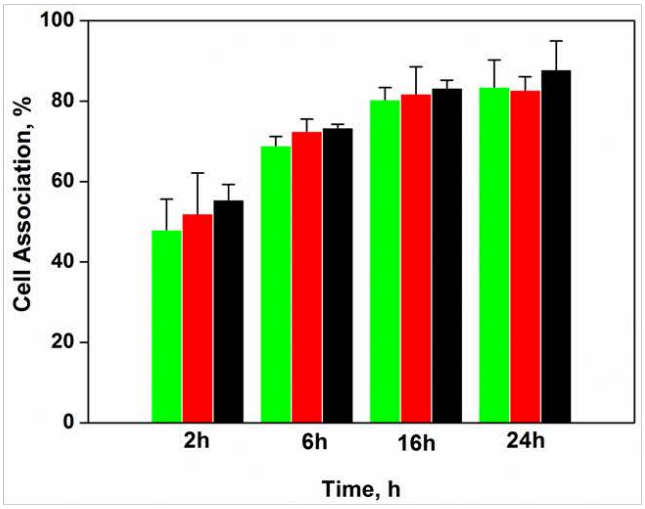
Cell Association, %
100
80
60
40
20
0
2h
6h
16h
24h
Time, h

B

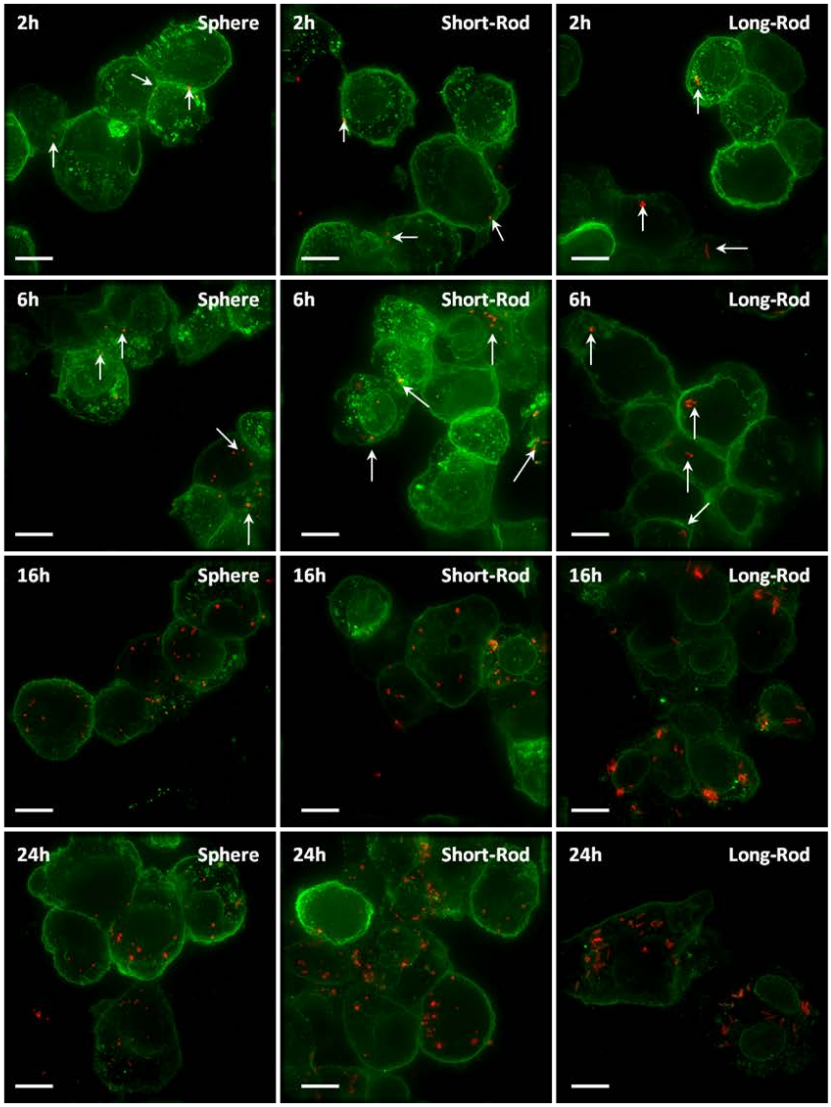
2h Sphere
2h Short-Rod
2h Long-Rod
6h Sphere
6h Short-Rod
6h Long-Rod
16h Sphere
16h Short-Rod
16h Long-Rod
24h Sphere
24h Short-Rod
24h Long-Rod

Figure 2. (A) Flow cytometry data showing the kinetics of cellular association of spherical and rod-shaped PMA_{SH} capsules with dTHP-1 cells over a 24 h incubation period at 37 ˚C. Data represent the mean ± standard error from three independent experiments, and at least 8000 cells were analyzed in each experiment. (B) Cellular association of capsules (red), as imaged by fluorescence deconvolution microscopy. The images are shown at maximum projection. Cell membranes were stained with AF488 WGA (green). Scale bars are 10 μm.

Next, the cellular internalization of PMA_{SH} capsules with different shapes was quantified by imaging flow cytometry, using a software-derived positive internalization factor that detects cells with internalized capsules. The results show the internalization levels of dTHP-1 cells increased slightly with increasing capsule AR. Cellular internalization levels of 90.6%, 96.0% and 96.8% were observed for spherical capsules, short rod-shaped capsules and long rod-shaped capsules, respectively (Figure 3, A-C). Despite the slight differences in the cellular internalization of different capsules by dTHP-1 cells, these differences are not sufficiently significant to suggest that internalization is capsule shape dependent.

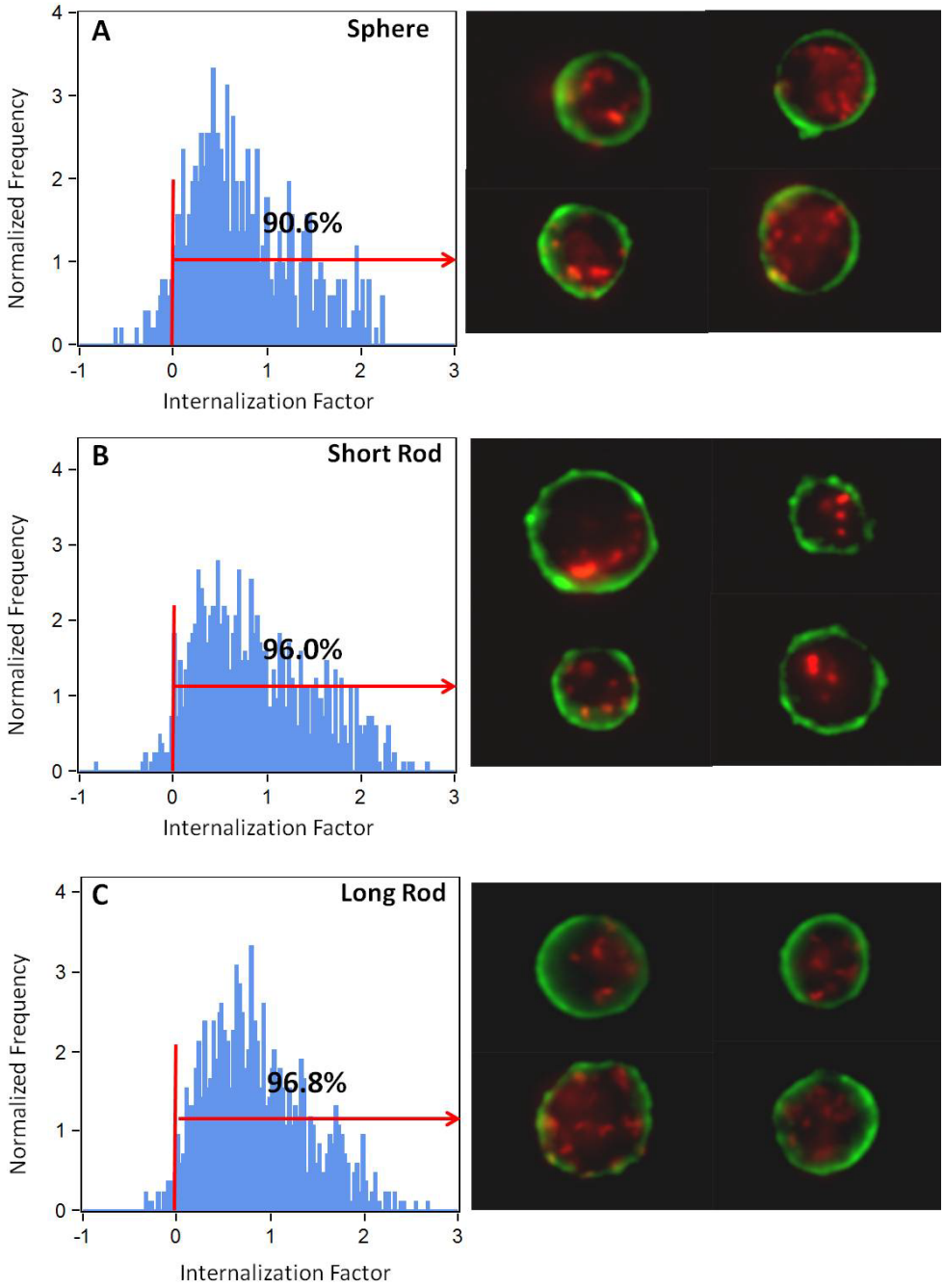

Figure 3. Imaging flow cytometry quantification of the internalization of AF633-labeled PMA_{SH} capsules of (A) spherical shape, (B) short-rod shape and (C) long-rod shape by dTHP-1 cells after 16 h incubation. The capsules are in red and the cell membrane (green) was stained with AF488 WGA. At least 5000 cells were analyzed in each experiment.

Cytokine Secretion. Cytokines are inflammatory mediators produced during an immunological response.[32] An increase in the release of cytokines indicates that the immune system is stimulated.[33] A previous study reported that gold nanoparticles could induce the production of different kinds of cytokines at different levels in dendritic cells, depending on the shape of the nanoparticles.[6] Therefore, we sought to examine whether the shape of PMA_{SH} capsules is a factor in mediating the inflammatory immune response of macrophages. The endotoxin level, which could contaminate samples and result in misleading inflammatory cytokine responses, was detected to be negligible (less than 0.05 EU/mL) for all the capsule samples. dTHP-1 cells were incubated with PMA_{SH} capsules at different capsule-to-cell ratios (0, 25, 50 and 100) for 24 h at 37 ˚C. The supernatants were collected and the levels of induced inflammatory cytokine (IL-1β, IL-6, IL-8, IL-18, TNF-α, and interferon gamma (IFN-γ)) were then examined by enzyme-linked immunosorbent assays. Our results show that significant changes in cytokine induction were observed mainly in dTHP-1 cells after treatment with PMA_{SH} capsules at a 100:1 capsule-to-cell ratio (Figure 4). This is in agreement with our previous study that dTHP-1 cells secreted higher levels of cytokines than monocytic THP-1 cells after exposure to PMA_{SH} nanoporous particles.[29] Meanwhile, it is notable that short rod-shaped PMA_{SH} capsules promoted a stronger increase in TNF-α (Figure 4A) and IL-8 secretion (Figure 4B) compared with spherical (1.7-fold in TNF-α and 2.1-fold in IL-8, $^{**}p < 0.005$) and long rod-shaped (2.8-fold in TNF-α and 2.0-fold in IL-8, $^{**}p < 0.005$) PMA_{SH} capsules in dTHP-1 cells. This indicates that the shape of PMA_{SH} capsules is an important factor in inducing TNF-α and IL-8 secretion in macrophage-like cells.

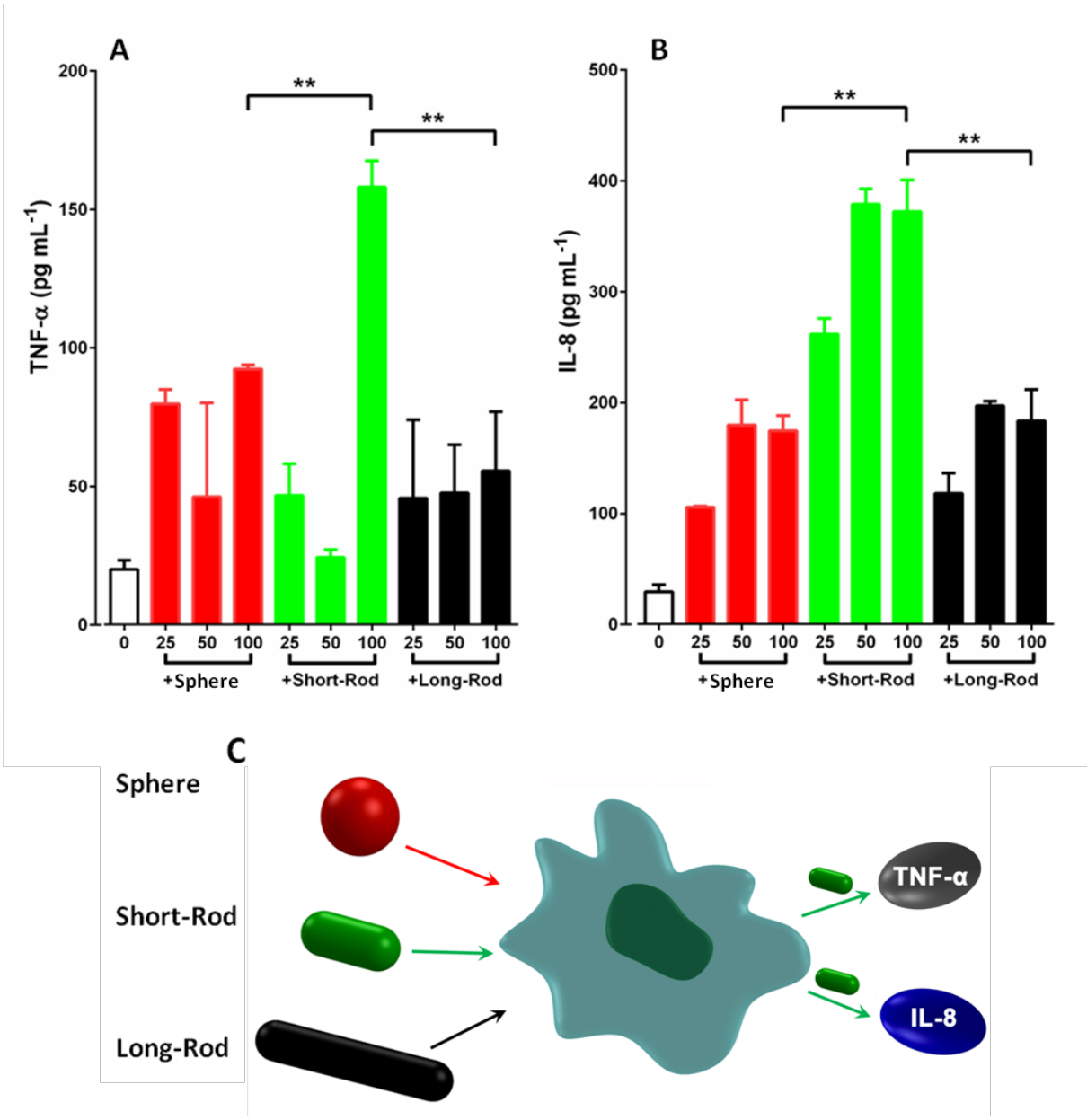

Figure 4. (A) TNF-α and **(B)** IL-8 secretion from dTHP-1 cells treated with PMA_{SH} capsules at capsule number-to-cell ratios of 0, 25, 50 and 100 for 24 h (red: spherical capsules; green: short rod-shaped capsules; black: long rod-shaped capsules). The capsule-to-cell ratio of 0 (white bar) refers to the base TNF-α and IL-8 secretion levels of the cells. Cytokine secretion was measured in triplicate from three independent experiments. Data are expressed as mean ± standard error;

p < 0.005 (one-way ANOVA Dunnett's multiple comparison test). (C**) Schematic illustration of the effect of polymer capsule shape on cytokine secretion in dTHP-1 cells.

Considering that the intracellular fate of the capsules may regulate the production of cytokines, we further investigated the intracellular localization of PMA_{SH} capsules with different shapes in dTHP-1 cells (Figure 5). The internalized capsules appeared to be mainly localized in the late endosomes and lysosomes, regardless of their shape. Since the capsules had the same intracellular fate and showed a similar extent of internalization (regardless of shape), these factors are unlikely to affect the production of cytokines in dTHP-1 cells.

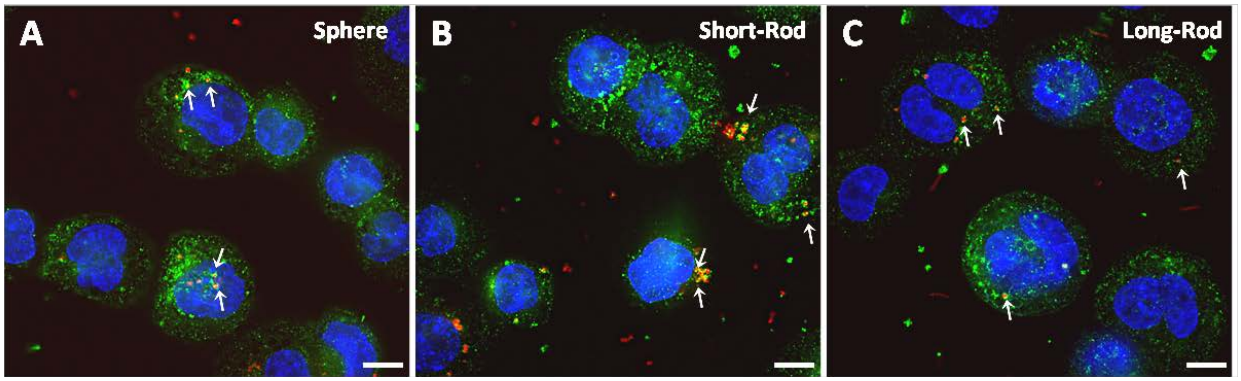

Figure 5. Deconvolution microscopy images of the cellular co-localization of AF633-fluorescently labeled PMA_{SH} capsules (marked by white arrows) of different shapes inside dTHP-1 cells (A: spherical PMA_{SH} capsules; B: short rod-shaped PMA_{SH} capsules; and C: long rod-shaped PMA_{SH} capsules). After 24 h incubation, the cells were immunostained with anti-LAMP 1 antibody (green), which binds to lysosomes. Cell nuclei (blue) were stained with Hoechst 33342. The images were taken at a single focal plane. Scale bars are 10 µm.

Notably, the capsules have different volumes as a consequence of their shapes and different ARs. Thus, we investigated whether differences in capsule volume affected the levels of TNF-α and IL-8 secretion in dTHP-1 cells. A previous study reported that spherical SiO_2 nanoparticles (D = 5 nm) stimulated higher levels of IL-8 production than larger sized particles (D = 100 nm).[34] Here, short rod-shaped capsules with a smaller volume stimulated higher levels of TNF-α and IL-8 compared to spherical and long rod-shaped capsules with larger volumes. To investigate the influence of volume, we evaluated TNF-α and IL-8 secretion by dTHP-1 cells with spherical capsules of 390 nm diameter (obtained from 235 nm SiO_2 templates), which have a similar internal volume to the short rod-shaped capsules. It was observed that the secretion of TNF-α and IL-8 induced by spherical 390 nm-diameter capsules at a capsule-to-cell ratio of 100:1 was lower (2.4-fold in TNF-α and 1.8-fold in IL-8, $^{**}p < 0.005$) than that induced by short rod-shaped capsules. Interestingly, there was no significant difference observed between the smaller (390 nm) and larger spherical capsules (670 nm) in terms of TNF-α and IL-8 secretion (Figure 6). This indicates that neither capsule volume nor size play a dominant role in determining cytokine secretion. This suggests that the secretion of TNF-α and IL-8 by macrophages is strongly dependent on polymer capsule shape. TNF-α and IL-8 are both inflammatory cytokines and are produced by various cells, including monocytes and macrophages, as a response to injury and infection. The secretion of TNF-α and IL-8, along with other cytokines, is normally induced by the presence of lipopolysaccharides, which bind to these cells via pattern recognition receptors.[35]

Further, the expression levels of other inflammatory cytokines, IL-1β, IL-6, IL-18 and IFN-γ, were also observed from dTHP-1 cells (Figure S6). Interestingly, our results show no significant difference in the production of these cytokines when different-shaped capsules with

the same capsule-to-cell ratio are used, indicating that the shape of PMA_{SH} capsules has a negligible impact on inducing these particular cytokines. The possible explanation is that the immune response is mediated via different cytokine pathways depending on particle shape, a funding which is also proposed by a previous study in of the case of gold nanoparticles with different shapes.[6] Due to the complexity of immune responses to external particles,[36] elucidation of the exact mechanism for the effect of polymer capsule shape on cytokine secretion requires further study.

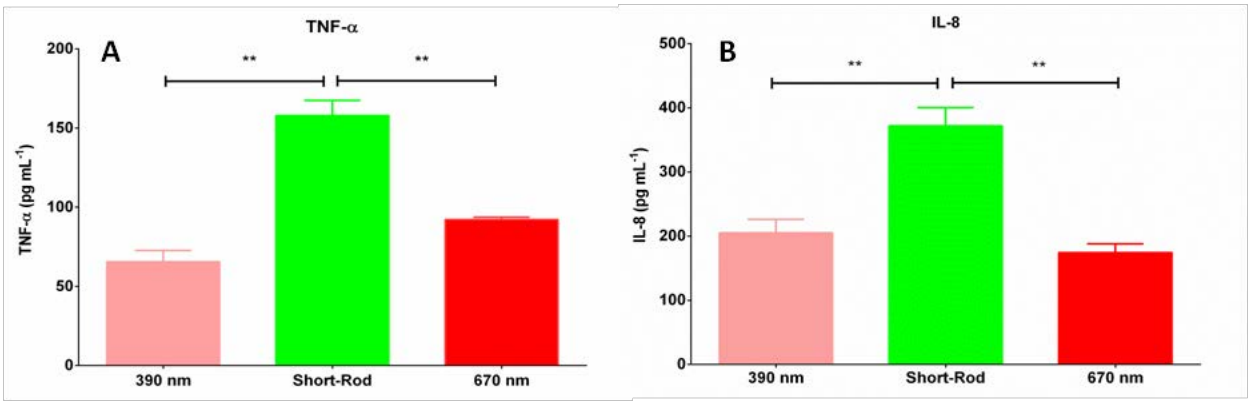

Figure 6. (A) TNF-α and (B) IL-8 secretion by dTHP-1 cells treated with PMA_{SH} capsules at 100:1 capsule number-to-cell ratio (390 nm: spherical capsules of 390 nm diameter; short-rod: short rod-shaped capsules; and 670 nm: spherical capsules of 670 nm diameter). Cytokine levels were measured in triplicate from three independent experiments. Data are expressed as mean ± standard error.

CONCLUSIONS

In conclusion, the immunological response of PMA_{SH} capsules by monocyte-derived macrophages based on cytokine secretion is dependent on the shape of the capsules. Our data show that the cellular association and internalization of PMA_{SH} capsules by macrophage-like dTHP-1 cells is shape independent. Importantly, our results demonstrate a shape-dependent activation of cytokine secretion by polymer capsules in dTHP-1 cells. Specifically, short rod-shaped (AR 2.2) PMA_{SH} capsules stimulated higher production of TNF-α and IL-8 compared with spherical (AR 1.0) and long rod-shaped (AR 7.4) capsules in dTHP-1 cells. Our findings suggest that polymer capsule shape is an important parameter for influencing the pro-inflammatory immunological behavior of macrophage-like cells. The cellular uptake and immunological response provide a practical way to explore the interactions between polymer capsules and the immune system, which in turn can guide the design of polymer capsules for application in vaccine delivery.

ASSOCIATED CONTENT

Supporting Information.

Supplementary information and figures. This material is available free of charge via the Internet at http://pubs.acs.org.

AUTHOR INFORMATION

Corresponding Author

*E-mail: fcaruso@unimelb.edu.au.

Author Contributions

The manuscript was written through contributions of all authors.

Notes

The authors declare no competing financial interest.

ACKNOWLEDGMENTS

This research was conducted through and funded by the Australian Research Council (ARC) Centre of Excellence in Convergent Bio-Nano Science and Technology (project number CE140100036). This work was also supported by the ARC under the Australian Laureate Fellowship (F.C., FL120100030), Discovery Early Career Researcher Award (Y.Y., DE130100488), and Super Science Fellowship (F.C., FS110200025) schemes. M.M. thanks the University of Melbourne for support through the McKenzie Fellowship. The authors thank Ka Fung Noi and Qiong Dai (the University of Melbourne) for assistance with capsule preparation. This work was performed in part at the Materials Characterisation and Fabrication Platform (MCFP) at the University of Melbourne and the Victorian Node of the Australian National Fabrication Facility (ANFF).

REFERENCES

(1) Zhao, L.; Seth, A.; Wibowo, N.; Zhao, C.-X.; Mitter, N.; Yu, C.; Middelberg, A. P. J. *Vaccine* **2014,** *32*, 327-337.

(2) Lim, E.-K.; Kim, T.; Paik, S.; Haam, S.; Huh, Y.-M.; Lee, K. *Chem. Rev.* **2015,** *115*, 327-394.

(3) Durán-Lobato, M.; Carrillo-Conde, B.; Khairandish, Y.; Peppas, N. A. *Biomacromolecules* **2014,** *15*, 2725-2734.

(4) Slupetzky, K.; Gambhira, R.; Culp, T. D.; Shafti-Keramat, S.; Schellenbacher, C.; Christensen, N. D.; Roden, R. B. S.; Kirnbauer, R. *Vaccine* **2007,** *25*, 2001-2010.

(5) Karkada, M.; Weir, G. M.; Quinton, T.; Fuentes-Ortega, A.; Mansour, M. *Vaccine* **2010,** *28*, 6176-6182.

(6) Niikura, K.; Matsunaga, T.; Suzuki, T.; Kobayashi, S.; Yamaguchi, H.; Orba, Y.; Kawaguchi, A.; Hasegawa, H.; Kajino, K.; Ninomiya, T.; Ijiro, K.; Sawa, H. *ACS Nano* **2013,** *7*, 3926-3938.

(7) Demento, S. L.; Cui, W.; Criscione, J. M.; Stern, E.; Tulipan, J.; Kaech, S. M.; Fahmy, T. M. *Biomaterials* **2012,** *33*, 4957-4964.

(8) De Geest, B. G.; Willart, M. A.; Hammad, H.; Lambrecht, B. N.; Pollard, C.; Bogaert, P.; De Filette, M.; Saelens, X.; Vervaet, C.; Remon, J. P.; Grooten, J.; De Koker, S. *ACS Nano* **2012,** *6*, 2136-2149.

(9) Ariga, K.; Yamauchi, Y.; Rydzek, G.; Ji, Q.; Yonamine, Y.; Wu, K. C. W.; Hill, J. P. *Chem. Lett.* **2014,** *43*, 36-68.

(10) Richardson, J. J.; Björnmalm, M.; Caruso, F. *Science* **2015,** *348*.

(11) De Rose, R.; Zelikin, A. N.; Johnston, A. P. R.; Sexton, A.; Chong, S.-F.; Cortez, C.; Mulholland, W.; Caruso, F.; Kent, S. J. *Adv. Mater.* **2008,** *20*, 4698-4703.

(12) Sexton, A.; Whitney, P. G.; Chong, S.-F.; Zelikin, A. N.; Johnston, A. P. R.; De Rose, R.; Brooks, A. G.; Caruso, F.; Kent, S. J. *ACS Nano* **2009,** *3*, 3391-3400.

(13) Jiang, W.; Kim, B. Y. S.; Rutka, J. T.; Chan, W. C. W. *Nat. Nanotechnol.* **2008,** *3*, 145-150.

(14) Cui, J.; De Rose, R.; Alt, K.; Alcantara, S.; Paterson, B. M.; Liang, K.; Hu, M.; Richardson, J. J.; Yan, Y.; Jeffery, C. M.; Price, R. I.; Peter, K.; Hagemeyer, C. E.; Donnelly, P. S.; Kent, S. J.; Caruso, F. *ACS Nano* **2015,** *9*, 1571-1580.

(15) Gratton, S. E. A.; Ropp, P. A.; Pohlhaus, P. D.; Luft, J. C.; Madden, V. J.; Napier, M. E.; DeSimone, J. M. *Proc. Natl. Acad. Sci. U.S.A.* **2008,** *105*, 11613-11618.

(16) Xie, J.; Xu, C.; Kohler, N.; Hou, Y.; Sun, S. *Adv. Mater.* **2007,** *19*, 3163-+.

(17) Win, K. Y.; Feng, S. S. *Biomaterials* **2005,** *26*, 2713-2722.

(18) Banquy, X.; Suarez, F.; Argaw, A.; Rabanel, J. M.; Grutter, P.; Bouchard, J. F.; Hildgen, P.; Giasson, S. *Soft Matter* **2009,** *5*, 3984-3991.

(19) Cui, J.; De Rose, R.; Best, J. P.; Johnston, A. P. R.; Alcantara, S.; Liang, K.; Such, G. K.; Kent, S. J.; Caruso, F. *Adv. Mater.* **2013,** *25*, 3468-3472.

(20) Nakanishi, W.; Minami, K.; Shrestha, L. K.; Ji, Q.; Hill, J. P.; Ariga, K. *Nano Today* **2014,** *9*, 378-394.

(21) Truong, N. P.; Whittaker, M. R.; Mak, C. W.; Davis, T. P. *Expert Opin. Drug Deliv.* **2015,** *12*, 129-142.

(22) Wang, J.; Yang, G.; Wang, Y.; Du, Y.; Liu, H.; Zhu, Y.; Mao, C.; Zhang, S. *Biomacromolecules* **2015,** *16*, 1987-1996.

(23) Chithrani, B. D.; Ghazani, A. A.; Chan, W. C. W. *Nano Lett.* **2006,** *6*, 662-668.

(24) Huang, X. L.; Teng, X.; Chen, D.; Tang, F. Q.; He, J. Q. *Biomaterials* **2010,** *31*, 438-448.

(25) Shimoni, O.; Yan, Y.; Wang, Y.; Caruso, F. *ACS Nano* **2013,** *7*, 522-530.

(26) Muñoz Javier, A.; Kreft, O.; Semmling, M.; Kempter, S.; Skirtach, A. G.; Bruns, O. T.; del Pino, P.; Bedard, M. F.; Rädler, J.; Käs, J.; Plank, C.; Sukhorukov, G. B.; Parak, W. J. *Adv. Mater.* **2008,** *20*, 4281-4287.

(27) Hutter, E.; Boridy, S.; Labrecque, S.; Lalancette-Hébert, M.; Kriz, J.; Winnik, F. M.; Maysinger, D. *ACS Nano* **2010,** *4*, 2595-2606.

(28) Chanput, W.; Mes, J. J.; Wichers, H. J. *Int. Immunopharmacol.* **2014,** *23*, 37-45.

(29) Yan, Y.; Gause, K. T.; Kamphuis, M. M.; Ang, C.-S.; O'Brien-Simpson, N. M.; Lenzo, J. C.; Reynolds, E. C.; Nice, E. C.; Caruso, F. *ACS Nano* **2013,** *7*, 10960-10970.

(30) Kuijk, A.; van Blaaderen, A.; Imhof, A. *J. Am. Chem. Soc.* **2011,** *133*, 2346-2349.

(31) Zelikin, A. N.; Li, Q.; Caruso, F. *Chem. Mater.* **2008,** *20*, 2655-2661.

(32) Hu, Q.; Wu, M.; Fang, C.; Cheng, C.; Zhao, M.; Fang, W.; Chu, P. K.; Ping, Y.; Tang, G. *Nano Lett.* **2015,** *15*, 2732-2739.

(33) Mottram, P. L.; Leong, D.; Crimeen-Irwin, B.; Gloster, S.; Xiang, S. D.; Meanger, J.; Ghildyal, R.; Vardaxis, N.; Plebanski, M. *Mol. Pharm.* **2007,** *4*, 73-84.

(34) Lim, D.-H.; Jang, J.; Kim, S.; Kang, T.; Lee, K.; Choi, I.-H. *Biomaterials* **2012,** *33*, 4690-4699.

(35) Stanley, A. C.; Lacy, P. *Physiology (Bethesda, Md.)* **2010,** *25*, 218-29.

(36) Smith, D. M.; Simon, J. K.; Baker Jr, J. R. *Nat. Rev. Immunol.* **2013,** *13*, 592-605.

Table of Contents Image